

DOI: 10.1070/QEL16069

Features of the electron density dynamics in the filamentation of femtosecond laser radiation in air at elevated pressure

P.A. Chizhov, V.V. Bukin, A.A. Ushakov, S.V. Garnov

Abstract. **The electron density in the plasma channel of a femtosecond filament in air at pressures from 1 to 7 atm is measured at different instants, starting from the ionisation onset and up to several hundreds of picoseconds after it. The initial electron density is found to increase sharply in the pressure range of 3–4 atm. The plasma channel diameter is found to decrease with an increase in pressure from 3 to 7 atm.**

Keywords: *femtosecond lasers, filamentation, interferometry.*

1. Introduction

The femtosecond laser plasma has been investigated in the recent decades. In particular, the filamentation of ultrashort laser beams has been analysed [1]. Femtosecond filamentation at a distance of several tens of meters was observed for the first time in [2]. The filamentation is the result of nonlinear optical interaction of high-power femtosecond laser pulses with a transparent medium. During self-focusing with an increase in the laser beam intensity to the photoionisation threshold, a laser plasma is formed; the defocusing in the latter limits a further rise of intensity in the nonlinear focus. The dynamic balance between the Kerr self-focusing and plasma defocusing leads to the formation of an extended plasma channel.

The peak values of the electron density for filamentation in air under atmospheric pressure, obtained by numerical simulation [3–5] and in measurements performed by different methods, including optical sensing [6, 7] and plasma fluorescence imaging [8], were found to be 10^{14}–10^{17} cm^{-3}, depending on the focusing parameters and laser pulse characteristics.

We performed a study by transmission interferometry. This technique allows one to estimate the electron density dynamics during several hundreds of picoseconds after ionisation, when the plasma density is still sufficiently high to detect reliably the phase shift [9, 10]. The experiments (see below) showed the reliably observed phase shift to be ~2 mrad, a value corresponding to a plasma density of $\sim 10^{16}$ cm^{-3} for a channel ~100 μm in diameter. Since electrons may recombine via many different mechanisms, the decay of the plasma channel can be studied under different conditions to reveal the contributions of these mechanisms. One of the parameters that can easily be varied and, at the same time, may affect significantly the filamentation character is gas pressure [11]. In this paper, we report the results of studying the influence of gas pressure on the electron density in the plasma channel formed during laser beam filamentation in air.

2. Experimental

A schematic of the experimental setup is shown in Fig. 1. A high-intensity femtosecond laser pulse [E = 2.5 mJ, t = 150 fs (FWHM), D = 12 mm (1/e^2)] formed a plasma channel when

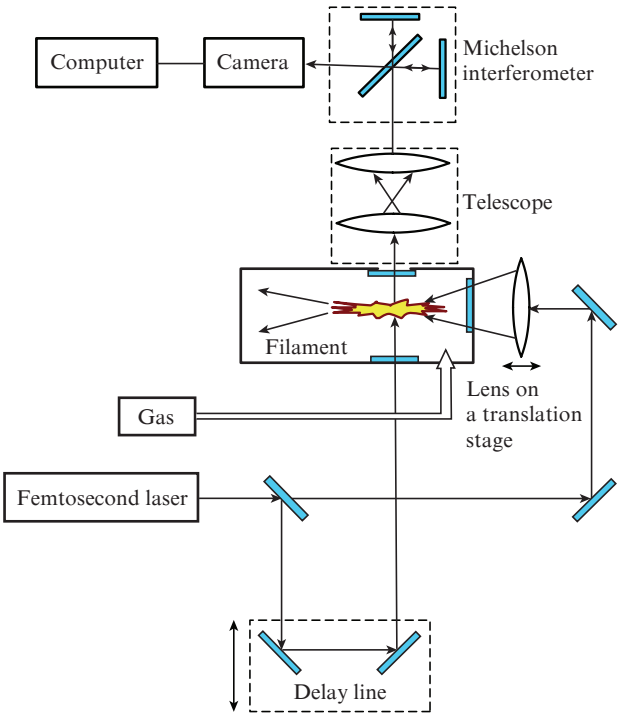

Figure 1. Schematic of the experimental setup.

P.A. Chizhov A.M. Prokhorov General Physics Institute, Russian Academy of Sciences, ul. Vavilova 38, 119991 Moscow, Russia;
e-mail: pvch@inbox.ru;
V.V. Bukin, S.V. Garnov A.M. Prokhorov General Physics Institute, Russian Academy of Sciences, ul. Vavilova 38, 119991 Moscow, Russia; National Research Nuclear University 'MEPhI', Kashirskoe sh. 31, 115409 Moscow, Russia;
e-mail: vladimir.bukin@gmail.com, svgarnov@mail.ru;
A.A. Ushakov A.M. Prokhorov General Physics Institute, Russian Academy of Sciences, ul. Vavilova 38, 119991 Moscow, Russia; Department of Physics, M.V. Lomonosov Moscow State University, Vorob'evy Gory, 119991 Moscow, Russia;
e-mail: ushakov.aleksandr@physics.msu.ru

Received 16 March 2016
Kvantovaya Elektronika **46** (4) 332–334 (2016)
Translated by Yu.P. Sin'kov

focused by a lens (f = 50 cm). The pulse repetition rate was 10 Hz. Plasma luminescence in a region about 2 cm long was visually observed under atmospheric pressure. The plasma channel was formed in a high-pressure chamber; the laser beam propagation length in the chamber to the focus was about 40 cm. The channel was transilluminated by a weak probe pulse of the same laser at the ionisation onset of the medium or at some other instant, controlled by an optical delay line. Series of interference patterns with plasma channel transillumination (signal) and without it (background) were recorded by a CMOS camera (Basler acA2040-25gm-NIR, 1″ 2048 × 2048); the plasma channel was imaged onto the camera array by a telescope.

We experimentally investigated the plasma channel region spaced from the geometric focus of the lens at a distance of ~1 cm (in the direction toward the focusing lens), which corresponded to the brightest part or the filament at atmospheric pressure. The presence of a phase object (plasma channel) on the test beam path changed the interference pattern. The interference patterns were processed using Fourier filtering to select the mean difference between the background and signal phase distributions, corresponding to the plasma phase additive [12]. Then, on the assumption of cylindrical symmetry of the plasma, the change in the refractive index was calculated based on this phase additive and the electron density was found (within the Drude model). The data processing technique used by us made it possible to record phase variations as small as ~2–3 mrad.

3. Results

Figure 2 shows an example of phase additive distribution in the probe beam, obtained by processing interference patterns. One can see well a plasma channel with a diameter of ~100 μm. The laser beam propagates from the right to the left. The plasma-induced phase shift is ~100 mrad. This distribution corresponds to the initial stage of plasma channel formation.

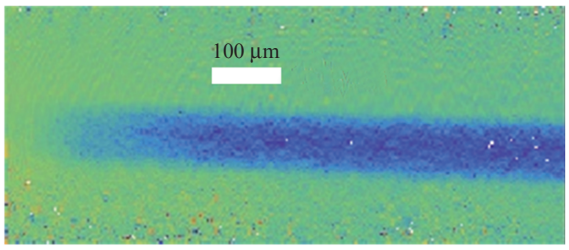

Figure 2. Example of a two-dimensional phase shift distribution over the plasma channel immediately after ionisation.

Figure 3 presents a pressure dependence of the initial peak electron density in the plasma channel, which indicates that the electron concentration in the plasma channel increases with an increase in pressure; this rise in density is highly nonuniform. In particular, the density is almost doubled with an increase in pressure from 3 to 4 atm.

Figure 4 shows electron density profiles in a filament cross section for air pressures of 2, 3, 4 and 6 atm, recorded 1 ps after the ionisation. The FWHMs of the profiles are 90 μm for pressures of 2 and 3 atm and about 75 and 65 μm for 4 and 6 atm, respectively. It should be noted that the channel diameter (as well as the peak electron density) varies only slightly in the range of 1–3 atm; however, a significant change is observed at a pressure of 4 atm. The further increase in the peak electron density is accompanied by a decrease in the plasma-channel diameter.

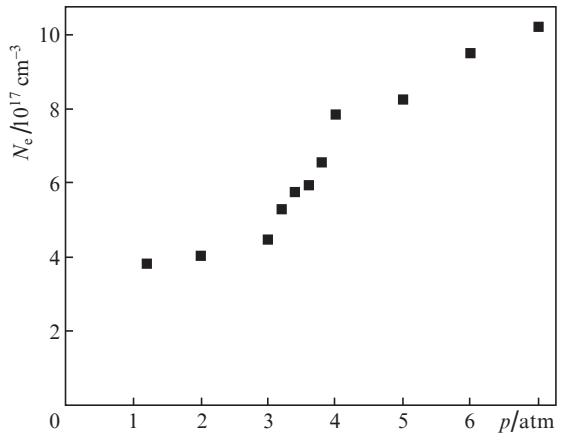

Figure 3. Dependence of the initial peak electron density in a plasma channel in air on pressure.

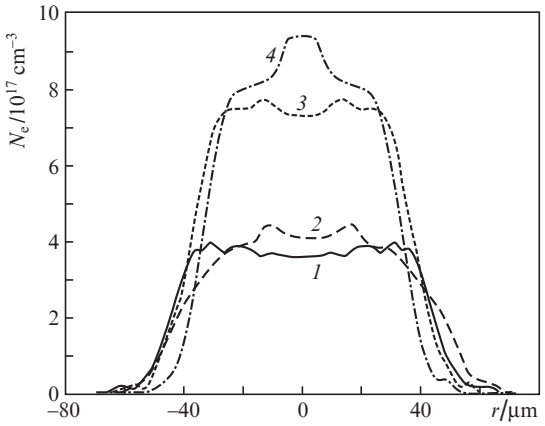

Figure 4. Electron density profiles in a plasma channel at pressures of (*1*) 2, (*2*) 3, (*3*) 4 and (*4*) 6 atm, recorded 1 ps after the ionisation.

In the pressure range of 1–10 atm, the refractive index of the medium is $n_0 \approx 1$, and the increase in nonlinear refractive index n_2 is directly proportional to pressure. For example, the following dependences of n_0 and n_2 for air at a wavelength λ = 1 μm were reported in [4]: $n_0 \approx 1 + 10^{-23}N_a$ and n_2 [cm^2 W^{-1}] $\approx 2 \times 10^{-38}N_a$, where N_a is the concentration of gas atoms [cm^{-3}]. Thus, the critical power $P_{cr} = \lambda^2/(2\pi n_0 n_2)$ in the first approximation is proportional to $1/N_a$ and decreases with an increase in pressure. On the other hand, for the same laser beam intensity I, the ionisation probability of gas atoms $w(I)$ remains the same, and the electron density $N_e \sim w(I)N_a$ linearly increases with an increase in pressure. At the plasma frequency $\omega_p^2 = 4\pi e^2 N_e/m_e$, the change in the refractive index caused by the plasma formation ($\Delta n_p \approx \frac{1}{2}(\omega_p/\omega)^2$) is proportional to N_e and N_a. Thus, in the first approximation, both focusing and defocusing are proportional to the gas pressure, the intensity corresponding to $n_2 = \Delta n_p$ remains the same, and the electron density is expected to

rise linearly. At the same time, $I \propto P_{cr}/S$ (S is the filament cross section area); therefore, under conditions of elevated pressure and reduced critical power of focusing, one must reduce S (i.e., the filament diameter) [13].

Our results are in qualitative agreement with the above considerations about the increase in the electron density and decrease in the plasma-channel diameter. However, as can be seen in Fig. 3, the electron density nonlinearly depends on pressure, and the channel parameters change sharply at pressures of 3–4 atm. The above explanation of the change in the channel parameters is fairly rough and does not take into account, e.g., the evolution of the femtosecond laser pulse during its propagation and the inertia of the response of the medium. In addition, the beam focusing by the lens also affects the channel. Note that, in view of the sharply nonlinear dependence of the gas ionisation probability on intensity, even small variations in equilibrium intensity change considerably the plasma electron density in the channel. On the whole, based on the experimental results, we can state that the equilibrium intensity decreases with an increase in pressure. Note also that the channel parameters were observed at only one point. The plasma channel has different lengths at different pressures, which may lead to displacement of the observed channel region from the region of maximum density and, correspondingly, affect the measured values of parameters.

Figure 5 shows experimental time dependences of the peak electron density on linear and logarithmic scales at plasma channel decay in air for pressures of 1–7 atm. It can be seen that the decay rate increases with an increase in pressure. For example, at a pressure of 3 atm, at the initial plasma channel parameters (diameter and electron density) close to those at a pressure of 1 atm, the electron recombination rate is much higher. We did not measure the electron temperature, which is the main parameter for calculating the probabilities of recombination mechanisms [10]. However, even at fixed initial plasma parameters, one would expect the decay rate to increase due to the increase in the collision frequency with an increase in pressure.

Thus, our study of the decay dynamics of femtosecond filament plasma channel revealed a monotonic increase in the electron recombination rate with an increase in gas pressure. A sharp rise in the initial electron density was observed in the pressure range of 3–4 atm. This rise is accompanied by a significant decrease in the channel diameter.

Acknowledgements. This work was supported by the 'Extreme Laser Radiation: Physics and Fundamental Applications' programme of the Presidium of the Russian Academy of Sciences, the Russian Foundation for Basic Research (Grant Nos 15-02-99630 and 15-32-20966) and the RF President's Grant Council (Support to the Leading Scientific Schools programme, Grant No. NSh-9695.2016.2).

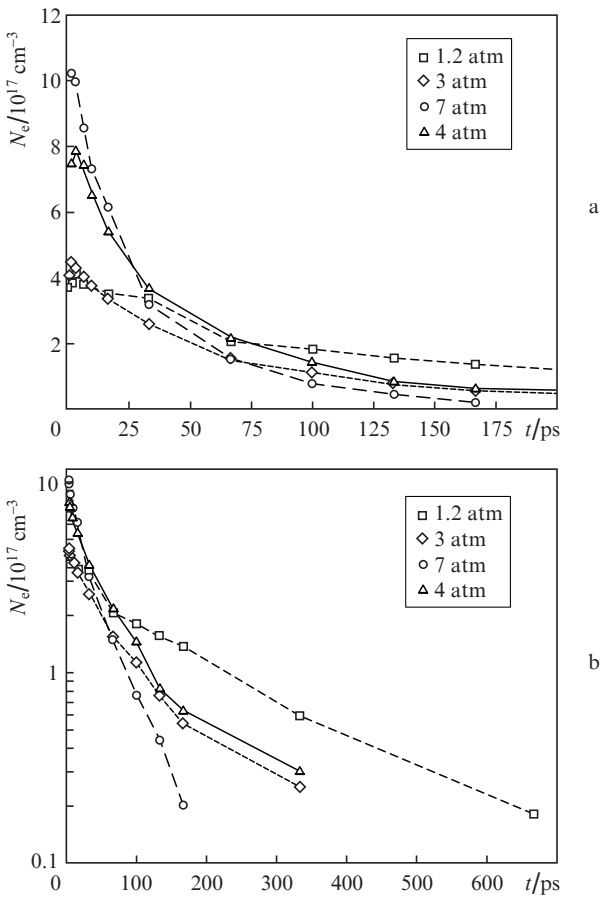

Figure 5. Time dependences of the peak electron density, starting with the onset of ionisation in the plasma channel of femtosecond filament in air at different pressures, on (a) linear and (b) logarithmic scales.

References

1. Couairon A., Mysyrowicz A. *Phys. Reports*, **441**, 47 (2007).
2. Braun A., Korn G., Liu X., Du D., Squier J., Mourou G. *Opt. Lett*., **20**, 73 (1995).
3. Mlejnek M., Wright E.M., Moloney J.V. *Opt. Lett*., **23**, 382 (1998).
4. Couairon A., Bergé L. *Phys. Plasmas*, **7**, 193 (2000).
5. Wu J., Antonsen T.M. *Phys. Plasmas*, **10**, 2254 (2003).
6. Rodriguez G., Valenzuela A.R., Yellampalle B., Schmitt M.J., Kim Ki-Yong. *J. Opt. Soc. Am. B*, **25**, 1988 (2008).
7. Théberge F., Liu W., Simard P.Tr., Becker A., Chin S.L. *Phys. Rev. E*, **74**, 036406 (2006).
8. Eisenmann S., Pukhov A., Zigler A. *Phys. Rev. Lett*., **98**, 155002 (2007).
9. Bukin V.V., Garnov S.V., Malyutin A.A., Strelkov V.V. *Kvantovaya Elektron*., **37** (10), 961 (2007) [*Quantum Electron*., **37** (10), 961 (2007)].
10. Bodrov S., Bukin V., Tsarev M., Murzanev A., Garnov S., Aleksandrov N., Stepanov A. *Opt. Express*, **19**, 6829 (2011).
11. Chizhov P., Bukin V., Garnov S. *Phys. Procedia*, **71**, 222 (2015).
12. Takeda M., Ina H., Kobayashi S. *J. Opt. Soc. Am*., **72** (1), 156 (1982).
13. Chin S.L., Wang T.J., Marceau C., Wu J., Liu J.S., Kosareva O., Panov N., Chen Y.P., Daigle J.F., Yuan S., Azarm A., Liu W.W., Seideman T., Zeng H.P., et al. *Laser Phys*., **22** (1), 1 (2012).